



**HAL**  
open science

## Thermal Stability of Thin hexagonal Boron Nitride grown by MOVPE on Epigraphene

Vishnu Ottapilakkal, Abhishek Juyal, Suresh Sundaram, A. Mballo, P. Vuong,  
Lin Beck, Grant Nunn, Yang Su, Annick Loiseau, Frédéric Fossard, et al.

► **To cite this version:**

Vishnu Ottapilakkal, Abhishek Juyal, Suresh Sundaram, A. Mballo, P. Vuong, et al.. Thermal Stability of Thin hexagonal Boron Nitride grown by MOVPE on Epigraphene. *Journal of Crystal Growth*, 2023, 603, pp.127030. 10.1016/j.jcrysgro.2022.127030 . hal-03818508

**HAL Id: hal-03818508**

**<https://hal.science/hal-03818508>**

Submitted on 20 Nov 2023

**HAL** is a multi-disciplinary open access archive for the deposit and dissemination of scientific research documents, whether they are published or not. The documents may come from teaching and research institutions in France or abroad, or from public or private research centers.

L'archive ouverte pluridisciplinaire **HAL**, est destinée au dépôt et à la diffusion de documents scientifiques de niveau recherche, publiés ou non, émanant des établissements d'enseignement et de recherche français ou étrangers, des laboratoires publics ou privés.

# Thermal stability of thin hexagonal boron nitride grown by MOVPE on epigraphene

V. Ottapilakkal<sup>a</sup>, A. Juyal<sup>a</sup>, S. Sundaram<sup>a,b,c</sup>, P. Vuong<sup>a</sup>, A. Mballo<sup>a</sup>, L. Beck<sup>d</sup>, G. Nunn<sup>d</sup>, Y. Su<sup>e</sup>, A. Loiseau<sup>f</sup>, F. Fossard<sup>f</sup>, J.S. Mérot<sup>f</sup>, D. Chapron<sup>g</sup>, T.H. Kauffmann<sup>g</sup>, J.P. Salvestrini<sup>a,b,c</sup>, P.L. Voss<sup>a,b</sup>, W.A. de Heer<sup>d</sup>, C. Berger<sup>a,d,\*</sup>, A. Ougazzaden<sup>a,b,\*</sup>

<sup>a</sup> CNRS, IRL 2958 Georgia Tech - CNRS, 2 rue Marconi, 57070 Metz, France

<sup>b</sup> Georgia Institute of Technology, School of Electrical and Computer Engineering, Atlanta, GA 30332-0250, USA

<sup>c</sup> Georgia Tech-Lorraine, 2 rue Marconi, 57070 Metz, France

<sup>d</sup> Georgia Institute of Technology, School of Physics, Atlanta, GA 30332-0250, USA

<sup>e</sup> Georgia Institute of Technology, Material Science and Engineering, Atlanta, GA 30332-0250, USA

<sup>f</sup> Laboratoire d'Etude des Microstructures, ONERA-CNRS, Université Paris Saclay, F-92322 Châtillon, France

<sup>g</sup> Laboratoire Matériaux Optiques, Photonique et Systèmes (LMOPS), Université de Lorraine & CentraleSupélec, 57070 Metz, France

Passivating graphene with a layer of hexagonal boron nitride (hBN) is known to protect it from environment effects that degrade its mobility. However, growth of high-quality BN on graphene is challenging because of the lack of surface dangling bonds. Here, we report the growth of thin BN films (down to 10 nm) on monolayer epigraphene grown on silicon carbide single-crystal substrates using metal-organic vapor phase epitaxy (MOVPE). The BN film has continuous coverage on the epigraphene surface, with smooth morphology. Particles consisting of layered BN are also observed on the surface with a higher density at the step edges. High-Resolution Scanning Transmission Electron Microscopy (HRSTEM) reveals high structural quality BN layers, with a clean and abrupt interface with graphene. The BN/epigraphene/SiC heterostructure is stable up to high temperature (1550 °C), and annealing improves its crystallinity. These results show that MOVPE growth technique has a potential for large-scale production of BN fully coated graphene and high-temperature applications.

## 1. Introduction

Making the potential of graphene a reality as an electronic material requires its growth at large scale and lithographic patterning compatible with current industrial methods [1]. A remarkable feature of graphene is its stability in temperature and in harsh environment [2] that could be exploited for high power – high temperature devices. Epigraphene (EG) is graphene grown epitaxially on silicon carbide single crystal wafers [1,3]. It has excellent thermal stability (it is grown in the range 1400–2000 °C) and the SiC substrate is a semiconductor already largely used for high-power electronics [4] with a broad range of commercial applications. However, the electronic properties of graphene are sensitive to environmental contaminants from the air, lithography resists, or top dielectrics which act as scattering centers and result in reduced carrier mobility, typically  $6000 \text{ cm}^2 \text{V}^{-1} \text{s}^{-1}$  in field effect transistor (FET) devices [5,6]. Passivating graphene with structurally similar hexagonal

boron nitride (hBN) is the best-known solution to eliminate this environmental sensitivity [7]. The high thermal stability and the honeycomb structure with a small lattice mismatch (1.7 %) compared to iso-structural graphene make hBN ideal for graphene passivation. In addition, hBN can serve as top dielectric for graphene devices [7] with its 6 eV wide band gap [8] and a dielectric constant of about 4 [9].

Graphene sandwiched between mechanically transferred hBN shows improved mobility up to  $140,000 \text{ cm}^2 \text{V}^{-1} \text{s}^{-1}$  close to charge neutrality [7,10–13]. However, the mechanical transfer methods used to fabricate hBN/graphene heterostructures typically result in interfacial defects such as trapped impurities, gas-filled blisters [14], poor repeatability and small sizes. A large-scale compatible method is to directly grow hBN on graphene using conventional chemical vapor deposition (CVD) [15–17] or molecular beam epitaxy (MBE) [15,18], where the main challenge is the interface quality and large-scale uniform coverage [19].

Recently, wafer-scale growth of multilayer hBN on sapphire

\* Corresponding authors at: CNRS, IRL 2958 Georgia Tech - CNRS, 2 rue Marconi, 57070 Metz, France.

E-mail addresses: [claire.berger@cnrs.fr](mailto:claire.berger@cnrs.fr), [claire.berger@physics.gatech.edu](mailto:claire.berger@physics.gatech.edu) (C. Berger), [abdallah.ougazzaden@georgiatech-metz.fr](mailto:abdallah.ougazzaden@georgiatech-metz.fr) (A. Ougazzaden).

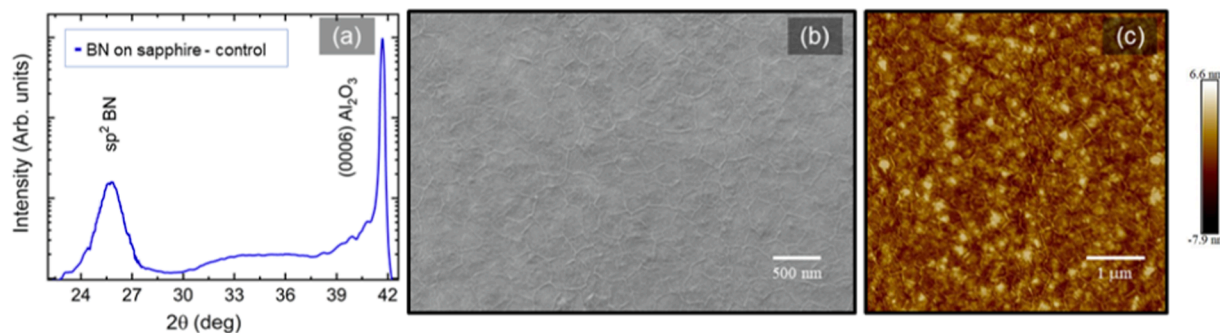


Fig. 1. Thin (10 nm) BN film on sapphire. (a) HR-XRD  $2\theta$ - $\omega$  scan (b) SEM image and (c) AFM image.

substrate using metal-organic vapor phase epitaxy (MOVPE) has been successfully demonstrated [20] and adapted to 20–50 nm thick BN films grown on epigraphene [21,22]. Entirely epitaxial BN/EG/SiC heterostructures were demonstrated. It is generally believed that the lack of dangling bond of graphene, its smooth surface and poor wettability makes it difficult to nucleate on the graphene surface [19]. The observed row-by-row, lateral epitaxial growth of BN on epigraphene [21] was analyzed through first-principles calculations, demonstrating one-dimensional nucleation-free-energy-barrier-less growth [21], where the atoms skid on the surface and anchor on the last row of the front growth. Although relatively thick (30–50 nm) BN films on epigraphene showed a clean and sharp epitaxial BN/EG interface and flat and ordered BN layers, cross-section transmission electron microscopy (TEM) reveals some misorientation in the top layers. As thinner hBN films over graphene are in any case desirable for field effect transistor applications, we have studied the fabrication of thin BN films on epigraphene. We present here results on the structural characterization of 10 nm thick BN films on epigraphene that indicate full coverage and excellent structural quality. Flat BN and pleated BN regions tens of  $\mu\text{m}^2$  in size are bordered by BN particles that are also layered BN. We finally demonstrate thermal stability of the heterostructure that withstands a 1550 °C annealing.

## 2. Experiments

Monolayer epigraphene was grown by thermal decomposition of the silicon terminated face of 6H SiC-(0001) using the confinement controlled sublimation method [3]. A polymer (photoresist AZ-5214E) was spin-coated on the bare SiC before thermal treatment [23]; this reduces the step heights and minimize the formation of bilayers at the steps [23] so that a monolayer graphene essentially covers the SiC continuously on the SiC terraces and steps like a carpet [3], similarly to epigraphene on the carbon face [24,25]. Samples were heated in a graphite crucible up to 1700 °C in an argon atmosphere. Details about epigraphene confinement growth can be found in Refs. [3,26]. Graphene quality was assessed by Raman spectroscopy (Fig. S1a) that shows typical graphene spectra with 2D peak widths ( $<40\text{ cm}^{-1}$ ) characteristic

of monolayers [3,24,27]. No disordered D peak is observed. Although bilayer graphene is occasionally observed (2D peak widths  $\sim 60\text{ cm}^{-1}$ ), Raman spectra taken at random locations on the epigraphene surface are very similar, showing essentially homogeneous epigraphene coverage on the stepped SiC (Fig. S1b).

The epigraphene samples were then transferred into the MOVPE growth chamber for BN growth. Triethylboron (TEB) and Ammonia ( $\text{NH}_3$ ) were used as precursors for boron and nitrogen, respectively. The precursors were alternately introduced to the growth chamber at a high temperature (1270 °C) under 85 mbar pressure. The detailed growth conditions have been reported elsewhere [20,21]. Note that the temperature is low enough so that no additional graphene layers are grown [3,26]. For each BN growth run, a 2-inch sapphire substrate was used as a control sample. BN was grown on epigraphene samples and on sapphire wafers under the same conditions in the same growth run. The growth was optimized to obtain down to 10 nm BN thickness on epigraphene. The structure of the heterostack was studied by high-resolution X-ray diffraction (HR-XRD) using a Panalytical X'pert Pro MRD system with  $\text{Cu K}\alpha$  radiation in triple-axis mode, Raman spectroscopy (Horiba Lab RAM HR laser wavelength 532 nm at spectroscopy platform of the LMOPS, Université de Lorraine & CentraleSupélec and Georgia Institute of Technology, Atlanta), Scanning Electron Microscopy (SEM) in image mode and Electron Back-scattering Diffraction (EBSD) mapping with a high-resolution field emission electron microscope (Tescan Mira3 XM FEG-SEM with EBSD), operating at 15 keV; High Resolution Scanning Transmission Microscopy (HR-STEM) using a probe-corrected ThermoFisher Scientific Titan G2 on cross-sections prepared by focused Ion Beam (FIB) and Atomic Force Microscopy (AFM – Park System) in non-contact mode.

The stability of the heterostructure stack was tested by annealing a 20 nm thick BN/EG/SiC sample at 1550 °C for 5 min. To prevent further graphene growth at these high temperatures, annealing was performed under high Si confinement condition (1 atm Ar, in a closed crucible, with an additional SiC chip in the face-to-face configuration). Details about epigraphene confinement growth can be found in Refs. [3,25,26].

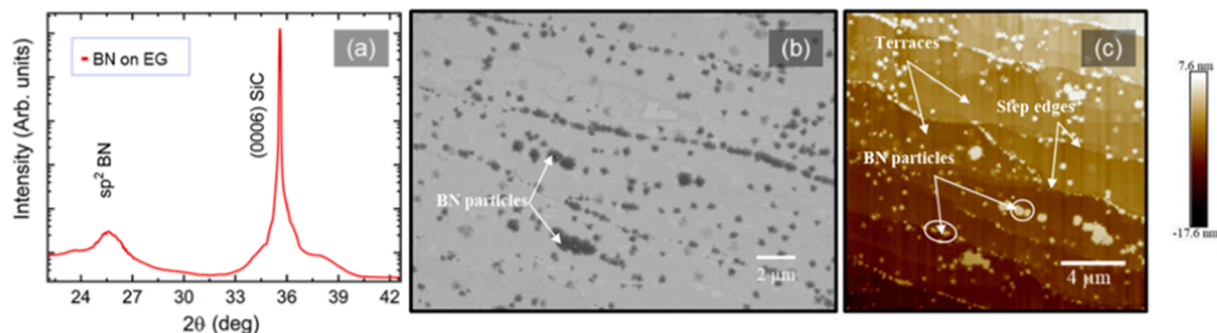
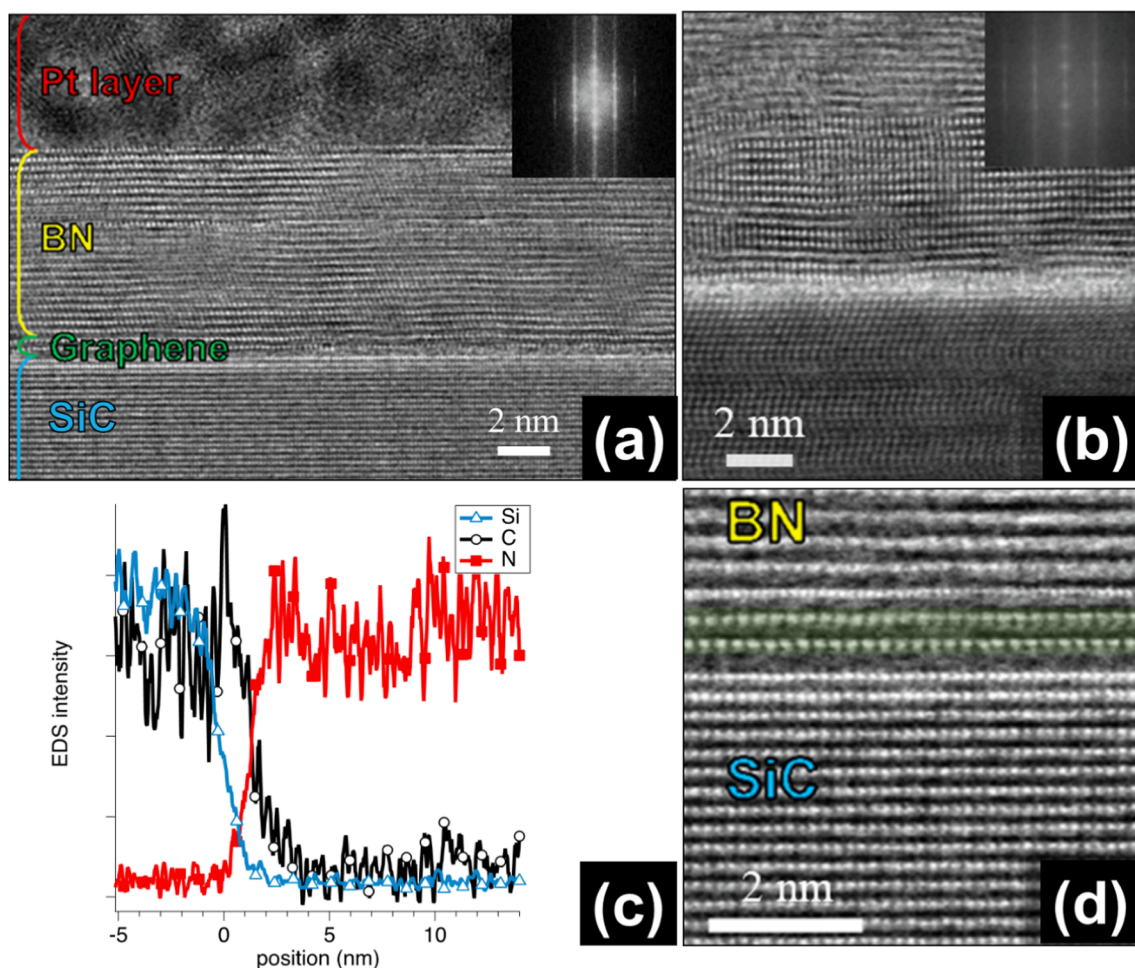


Fig. 2. Thin (10 nm) BN film on epigraphene. (a) HR-XRD  $2\theta$ - $\omega$  scan (b) SEM image and (c) AFM image.



**Fig. 3.** Cross-sectional TEM of BN/EG/SiC heterostructures, showing (a) a BN layer thickness of 10 nm on a 2-layer graphene (buffer + graphene) and inset is the Fast Fourier transform (FFT) of 10 nm BN showing ABC stacking insertions. (b) an AA' stacking (hexagonal phase) in 10 nm BN/EG. (c) Elemental EDS profiles of Si (blue), C (black) and N (red) across the BN/EG/SiC interfaces. At the location where both Si and N profiles vanish, the C profile displays a sharp peak over about 1 nm that is assigned to the graphene layers. N and C profiles are clearly anti correlated indicating an atomically sharp interface between the graphene layers and the first BN layer. The green color bilayer in (d) indicates graphene and the graphene- buffer layer (from in situ EDS analysis).

### 3. Results and discussion

#### 3.1. BN growth on sapphire – Control sample

Growth of BN on sapphire substrates serves as control sample for each growth run. The crystal structure of the BN control sample was examined by HR-XRD. The  $2\theta-\omega$  scan in Fig. 1a shows a broad peak at  $25.6^\circ$ , ascribed to  $sp^2$  BN (hexagonal or rhombohedral) and the sapphire (0006) peak at  $41.6^\circ$ , confirming the growth of BN on sapphire. The peak position corresponds to a BN interlayer spacing of 0.347 nm, in agreement with ref. [21] and consistent with that of hBN (0.333 nm) [28]. The increase in the layer spacing could be due to residual strain resulting from cooling after growth or turbostratic stacking [29].

The SEM and AFM image of Fig. 1b, c shows homogeneous coverage over the surface, with organized semi-hexagonal pleat patterns with an average domain size of about 300 nm and pleat height around 3–5 nm. The formation of pleats results from biaxial compressive strain due the difference in the thermal expansion coefficient between the BN and the underlying sapphire substrate [20,30,31]. These pleats confirm the presence of layered BN. The XRD and surface characterizations are similar to the previously reported BN growth on sapphire substrates [20].

#### 3.2. BN growth on monolayer EG

HR-XRD of the BN/EG/SiC heterostructure grown in the same run as the control sample on sapphire shown above presents essentially the same characteristics as BN grown on sapphire. HR-XRD  $2\theta-\omega$  scan in Fig. 2a shows a  $sp^2$  BN peak at the same location ( $25.6^\circ$ ) as growth on sapphire, indicating the same interlayer distance. The peak at  $35.8^\circ$  corresponds to the (0006) SiC substrate.

The surface morphology of this BN film grown on epigraphene was studied by SEM and AFM. A smooth (light grey) BN surface is observed in SEM over micron-sized epigraphene terraces with particles (dark grey) on the epigraphene coated step edges. The smooth surface and the absence of visible defects at the surface, as shown in Fig. 2b, supports that the BN film fully covers epigraphene. Individual Raman spectra recorded on the light and dark grey areas (Fig. S2) show similar spectra confirming uniformity of coverage. The signature pleats that appear on BN/sapphire are essentially not observed (Fig. 1b, Fig. 1c); these regions with non-pleated flat surfaces will require further investigation to distinguish between a fully relaxed BN film or the same compressive strain as the epigraphene it is grown on. Note that monolayer epigraphene on the Si-terminated face of SiC is locked epitaxially on the Si-face and therefore does not show pleating upon cooling from the growth temperature (Fig. S1b) [25]. Further studies will be needed to determine whether the absence of pleats in this case is due to the epitaxial

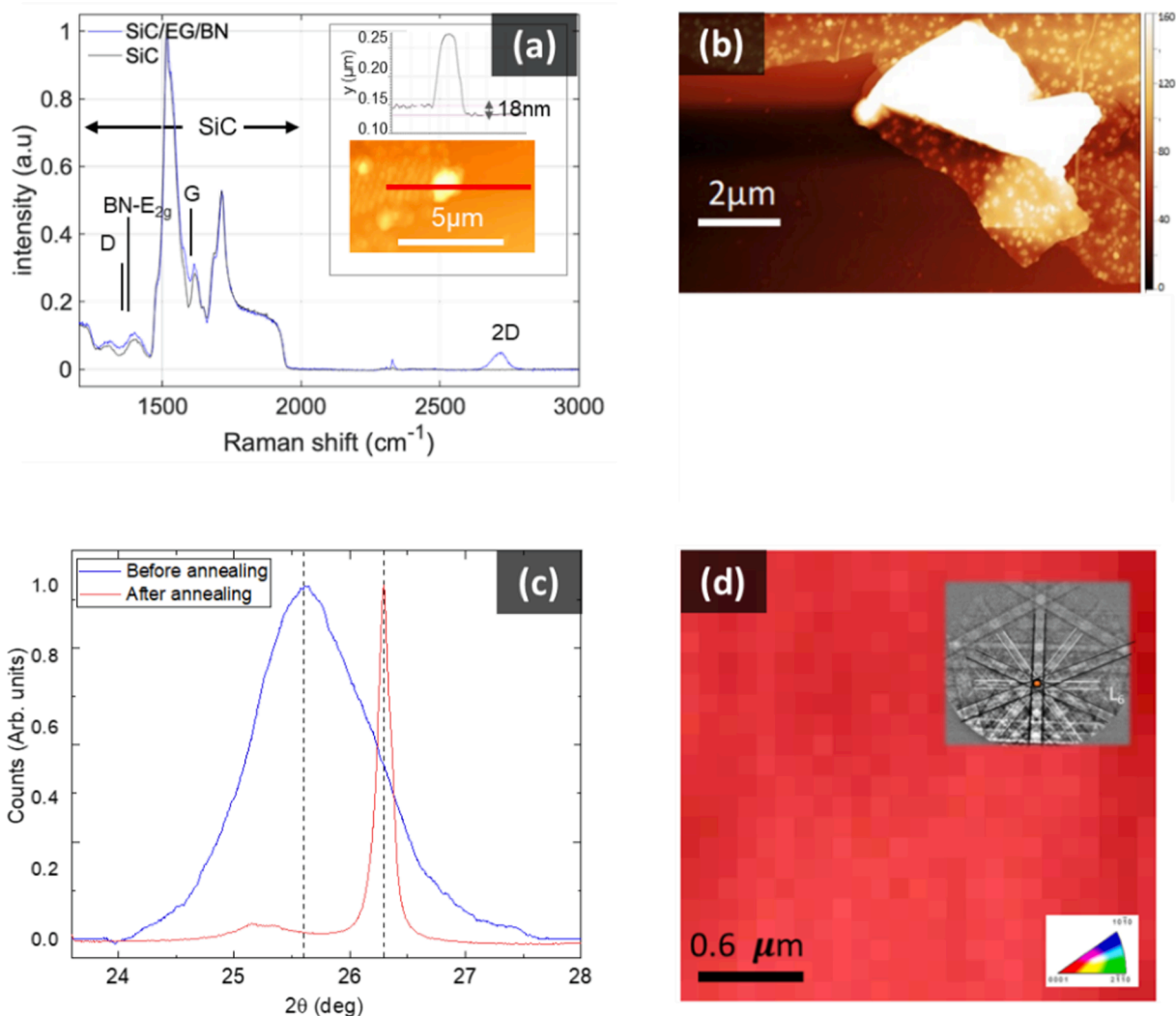


**Fig. 4.** High temperature annealed BN/EG/SiC heterostructure (1550 °C for 5 mins). (a) Raman spectroscopy of the heterostructures showing the characteristic graphene 2D and G peaks and the position of the BN- $E_{2g}$  peak (blue trace) and bare SiC reference substrate showing the SiC peaks (black trace). (inset) AFM topographic profile near a scratch, showing a BN thickness of 18 nm, consistent with the as-deposited BN thickness on this sample (the white particles are material plowed away on the side of the scratch and serve as a marker for the edge of the scratch). (b) AFM image with a torn folded BN/EG region, showing the cohesiveness of the film after annealing. (c) Normalized X-ray diffraction ( $2\theta - \omega$  scans) of BN/EG/SiC before (blue trace) and after (red trace) annealing. Annealed heterostructures shows a very well-defined peak at  $2\theta = 26.294$  deg. (d) EBSD inverse pole figure (IPF) maps superimposed by band contrast (BC) and corresponding legend of IPF map. Inset shows observed Kikuchi pattern with the 6-fold rotation axis of h-BN.

relationship between BN and epigraphene [21], or to fully relaxed BN layers. The AFM and SEM images in Fig. 2b-c show that the particles are more concentrated on the epigraphene-covered SiC step edges and sparsely distributed on its terraces [21]. Particles at the step edges are well understood in the nucleation-free-energy-barrier-less growth model of ref. [21], where B atoms skid on the surface and bind on the last row of the front growth. In this growth model, the step edge acts as a nucleation site, and two-dimensional BN growth propagates on the terraces. Localized strain variations and nucleation on defect and step edges or combination of these parameters can lead to the crumpled BN sheet formation at the edges [19].

HR-STEM studies on cross-sections prepared by Focused Ion Beam (FIB) confirm that the BN film exhibits a flat and layered structure with about 10 nm in thickness (Fig. 3a), in agreement with the nominal targeted thickness on epigraphene. The Fast Fourier transform pattern of 10 nm BN/EG shows AA' stacking, which corresponds to hexagonal phase of BN (Fig. 3b). In some regions of the samples a rhombohedral (ABC stacking) insertions were also observed. Fig. 3c shows the energy dispersive X-ray spectroscopy (EDS) profile of Si, C, and N K lines across

the BN/EG/SiC interfaces. The 1 nm shift between silicon and carbon extinction indicates the presence of graphene between SiC and BN. EDS mapping of the hetetostack is shown in Fig. S3. The 2-layer graphene (buffer layer [25] topped by a monolayer epigraphene) is also highlighted in Fig. 3d. We have also occasionally observed curving of the entire BN stack (Fig. S4) which we believe is associated with the particles observed in SEM and AFM (Fig. 2b, c). Previous Electron Energy Loss Spectroscopy (EELS) experiments indicated that the BN layers in these particles was in  $sp^2$  configuration [21], therefore has a layered structure, which is also clearly demonstrated here.

### 3.3. High temperature stability of the BN/EG/SiC heterostructure

The Raman spectrum of the annealed BN/EG/SiC in Fig. 4a (blue trace) shows the graphene peaks (2D peak at  $2734 \text{ cm}^{-1}$  and G peak at  $1600 \text{ cm}^{-1}$ ) and large SiC peaks (measured spectral range up to  $2000 \text{ cm}^{-1}$ , black trace). The large fluorescence observed in the Raman spectrum before the high temperature annealing that prevented the resolution of the graphene and BN peak (only the large SiC peaks were visible),

is not observed post annealing. The width of the 2D peak (FWHM = 50  $\text{cm}^{-1}$ ) confirms that no additional layers were grown during the post BN-growth annealing. The BN  $E_{2g}$  (1373  $\text{cm}^{-1}$ ) and the graphene D-peak (1350  $\text{cm}^{-1}$ ) locations are indicated. The BN and graphene D-peaks are very close and, superimposed to the SiC features, hence cannot be resolved. However, note that the graphene D-peak was undetectable in the as-grown samples, and it was previously demonstrated that the MOVPE process does not damage graphene [21]; therefore the small observed bump above the SiC peak around 1370  $\text{cm}^{-1}$  can reasonably be attributed to BN. The typical BN pleat and particle structure observed on the as-grown surface is seen also after annealing. A scratch test performed after annealing (inset Fig. 4a) indicates a step height of about 18 nm, compatible with the thickness of the as-deposited BN. This supports the presence of BN after annealing on the heterostack, which is confirmed by the AFM image of Fig. 4b, where the film was locally torn and folded over, demonstrating its cohesiveness after annealing.

XRD ( $2\theta - \omega$  scans) in Fig. 4c shows a well-defined peak at  $2\theta = 26.294^\circ$ , shifted compared to the as-grown peak ( $2\theta = 25.6^\circ$ ) and corresponding to interatomic distances  $d = 0.339$  nm, close to that of hBN (0.333 nm) [28]. The interlayer spacing suggests a residual strain of 2%, in agreement with the literature [29]. The width of the diffraction peak indicates an ordered stack on a distance roughly estimated between 25 and 30 nm, which is compatible with the nominal BN thickness. The small intensity shoulder centered around  $2\theta \approx 25.25^\circ$  may be related to the remaining particles made of strongly bended  $sp^2$  BN.

A crystallographic orientation mapping of the annealed stack was performed using EBSD mapping. Fig. 4d shows the inverse pole figure (IPF) map (scan step size of  $0.1 \times 0.1 \mu\text{m}$ ) superimposed with band contrast [32]. The signal from 6H-SiC single crystal was subtracted as a uniform background correction across the whole surface. The Kikuchi pattern, shown in the inset of Fig. 4d, can be indexed with hexagonal BN, with the [0001] axis out of the plane. The EBSD mapping shows a very uniform crystallographic orientation, with little tilt (confirming prior rocking curve measurements [21]), but, most interestingly, little azimuthal misorientation over  $2.5 \mu\text{m}$ .

In conclusion, XRD, AFM, Raman spectroscopy and EBSD results all converge and show that the BN/EG/SiC heterostack is stable at high temperature. The high temperature annealing reduces the BN interlayer distance, improves crystallinity and the graphene quality is preserved.

#### 4. Conclusion

In summary, the growth of thin BN films on epigraphene was demonstrated down to 10 nm. The BN film has a homogenous and smooth morphology on large terraces with particles mostly on step edges. Cross-sectional high-resolution transmission electron microscopy confirms the high-quality of the BN film on the epigraphene surface. The heterostack is stable up to very high temperature (1550  $^\circ\text{C}$ ) and the annealed structures show an improvement of the BN quality. This study confirms that thin-layer BN quality resulting from the MOVPE is promising for graphene-based thin body FET devices.

#### Credit authorship contribution statement

**V. Ottapilakkal:** Investigation, Writing – original draft, Visualization, Methodology. **A. Juyal:** Writing – original draft, Investigation, Methodology. **S. Sundaram:** Writing – review & editing, Supervision, Methodology, Conceptualization. **P. Vuong:** Investigation. **A. Mballo:** Investigation. **L. Beck:** Investigation. **G. Nunn:** Investigation. **Y. Su:** Investigation, Visualization. **A. Loiseau:** Writing – review & editing. **F. Fossard:** Visualization, Investigation. **J.S. Mérot:** Investigation. **D. Chapron:** Investigation. **T.H. Kauffmann:** Investigation. **J.P. Salvestrini:** Writing – review & editing. **P.L. Voss:** Writing – review & editing. **W.A. de Heer:** Conceptualization, Supervision, Writing – review & editing. **C. Berger:** Writing – review & editing, Supervision, Methodology, Conceptualization. **A. Ougazzaden:** Writing – review & editing,

#### Acknowledgments

This work is supported by a grant from the Agence Nationale de la Recherche (No ANR-19-CE24-0025). CB, AJ and AN acknowledge funding from the European Union Graphene Flagship grant agreements No. 696656 and No 785219. GN acknowledge funding from a Georgia Tech SP22 Seed Grant. This work was also made possible by the French American Cultural Exchange council through a Thomas Jefferson grant.

#### References

- [1] C. Berger, Z.M. Song, T.B. Li, X.B. Li, A.Y. Ogbazghi, R. Feng, Z.T. Dai, A. N. Marchenkov, E.H. Conrad, P.N. First, W.A. De Heer, Ultrathin Epitaxial Graphite: 2D Electron Gas Properties And a Route Toward Graphene-Based Nanoelectronics, *J. Phys. Chem. B* 108 (2004) 19912–19916.
- [2] J. Hicks, R. Arora, E. Kenyon, P.S. Chakraborty, H. Tinkey, J. Hankinson, C. Berger, W.A. de Heer, E.H. Conrad, J.D. Cressler, X-ray radiation effects in multilayer epitaxial graphene, *Appl. Phys. Lett.* 99 (2011) 232102.
- [3] W.A. de Heer, C. Berger, M. Ruan, M. Sprinkle, X. Li, Y. Hu, B. Zhang, J. Hankinson, E.H. Conrad, Large Area and Structured Epitaxial Graphene Produced by Confinement Controlled Sublimation of Silicon Carbide, *Proc. Nat. Acad. Sci.* 108 (2011) 16900–16905.
- [4] C.R. Eddy, D.K. Gaskill, Silicon Carbide as a Platform for Power Electronics, *Science* 324 (2009) 1398–1400.
- [5] S. Kim, J. Nah, I. Jo, D. Shahrjerdi, L. Colombo, Z. Yao, E. Tutuc, S.K. Banerjee, Realization of a high mobility dual-gated graphene field-effect transistor with Al<sub>2</sub>O<sub>3</sub> dielectric, *Appl. Phys. Lett.* 94 (2009).
- [6] Z. Guo, R. Dong, P.S. Chakraborty, N. Lourenco, J. Palmer, Y. Hu, M. Ruan, J. Hankinson, J. Kunc, J.D. Cressler, C. Berger, W.A. de Heer, Record Maximum Oscillation Frequency in C-Face Epitaxial Graphene Transistors, *Nano Lett.* 13 (2013) 942–947.
- [7] C.R. Dean, A.F. Young, I. Meric, C. Lee, L. Wang, S. Sorgenfrei, K. Watanabe, T. Taniguchi, P. Kim, K.L. Shepard, J. Hone, Boron Nitride Substrates for High-Quality Graphene Electronics, *Nat. Nanotechnol.* 5 (2010) 722–726.
- [8] K. Watanabe, T. Taniguchi, H. Kanda, Direct-bandgap properties and evidence for ultraviolet lasing of hexagonal boron nitride single crystal, *Nat. Mater.* 3 (2004) 404–409.
- [9] A. Laturia, M.L. Van de Put, W.G. Vandenberghe, Dielectric properties of hexagonal boron nitride and transition metal dichalcogenides: from monolayer to bulk, *npj 2D Mater. Appl.* 2 (2018) 6.
- [10] K.K. Kim, A. Hsu, X. Jia, S.M. Kim, Y. Shi, M. Dresselhaus, T. Palacios, J. Kong, Synthesis and Characterization of Hexagonal Boron Nitride Film as a Dielectric Layer for Graphene Devices, *ACS Nano* 6 (2012) 8583–8590.
- [11] M.S. Bresnehan, M.J. Hollander, M. Wetherington, M. LaBella, K.A. Trumbull, R. Cavalero, D.W. Snyder, J.A. Robinson, Integration of Hexagonal Boron Nitride with Quasi-freestanding Epitaxial Graphene: Toward Wafer-Scale, High-Performance Devices, *ACS Nano* 6 (2012) 5234–5241.
- [12] K.H. Lee, H.-J. Shin, J. Lee, I.-Y. Lee, G.-H. Kim, J.-Y. Choi, S.-W. Kim, Large-Scale Synthesis of High-Quality Hexagonal Boron Nitride Nanosheets for Large-Area Graphene Electronics, *Nano Lett.* 12 (2012) 714–718.
- [13] W. Min, J.S. Kyu, J. Won-Jun, K. Minwoo, P. Seong-Yong, K. Sang-Woo, K. Se-Jong, C. Jae-Young, R.R. S., S.Y. Jae, L. Sungjoo, A Platform for Large-Scale Graphene Electronics – CVD Growth of Single-Layer Graphene on CVD-Grown Hexagonal Boron Nitride, *Adv. Mater.* 25 (2013) 2746–2752.
- [14] D.G. Purdie, N.M. Pugno, T. Taniguchi, K. Watanabe, A.C. Ferrari, A. Lombardo, Cleaning Interfaces in Layered Materials Heterostructures, *Nat. Commun.* 9 (2018) 5387.
- [15] Z. Liu, L. Song, S. Zhao, J. Huang, L. Ma, J. Zhang, J. Lou, P.M. Ajayan, Direct Growth of Graphene/Hexagonal Boron Nitride Stacked Layers, *Nano Lett.* 11 (2011) 2032–2037.
- [16] J.M.P. Alaboson, Q.H. Wang, J.D. Emery, A.L. Lipson, M.J. Bedzyk, J.W. Elam, M. J. Pellin, M.C. Hersam, Seeding Atomic Layer Deposition of High-k Dielectrics on Epitaxial Graphene with Organic Self-Assembled Monolayers, *ACS Nano* 5 (2011) 5223–5232.
- [17] Y. Song, C. Zhang, B. Li, G. Ding, D. Jiang, H. Wang, X. Xie, Van der Waals epitaxy and characterization of hexagonal boron nitride nanosheets on graphene, *Nanoscale Res. Lett.* 9 (2014) 367.
- [18] D. Pierucci, J. Zribi, H. Henck, J. Chaste, M.G. Silly, F. Bertran, P. Le Fevre, B. Gil, A. Summerfield, P.H. Beton, S.V. Novikov, G. Cassabois, J.E. Rault, A. Ouerghi, Van der Waals Epitaxy of Two-Dimensional Single-Layer h-BN on Graphite by Molecular Beam Epitaxy: Electronic Properties and Band Structure, *Appl. Phys. Lett.* 112 (2018).
- [19] Y.-C. Lin, N. Lu, N. Perea-Lopez, J. Li, Z. Lin, X. Peng, C.H. Lee, C. Sun, L. Calderin, P.N. Browning, M.S. Bresnehan, M.J. Kim, T.S. Mayer, M. Terrones, J.A. Robinson, Direct Synthesis of van der Waals Solids, *ACS Nano* 8 (2014) 3715–3723.
- [20] X. Li, S. Sundaram, Y. El Gmili, T. Ayari, R. Puybaret, G. Patriarche, P.L. Voss, J. P. Salvestrini, A. Ougazzaden, Large-Area Two-Dimensional Layered Hexagonal Boron Nitride Grown on Sapphire by Metalorganic Vapor Phase Epitaxy, *Cryst. Growth Des.* 16 (2016) 3409–3415.
- [21] J. Gliotti, X. Li, S. Sundaram, D. Deniz, V. Prudkovskiy, J.-P. Turmaud, Y. Hu, Y. Hu, F. Fossard, J.-S. Mérot, A. Loiseau, G. Patriarche, B. Yoon, U. Landman,

A. Ougazzaden, C. Berger, W.A. de Heer, Highly Ordered Boron Nitride/  
Epigraphene Epitaxial Films on Silicon Carbide by Lateral Epitaxial Deposition,  
ACS Nano 14 (2020) 12962–12971.

- [22] J. Gigliotti, Integrated dielectrics for protection and gating of epitaxial graphene devices, Material Science and Engineering, PhD - Georgia Institute of Technology, Georgia Institute of Technology, 2017.
- [23] M. Kruskopf, D.M. Pakdehi, K. Pierz, S. Wundrack, R. Stosch, T. Dziomba, M. Götz, J. Baringhaus, J. Aprojanz, C. Tegenkamp, J. Lidzba, T. Seyller, F. Hohls, F. J. Ahlers, H.W. Schumacher, Comeback of epitaxial graphene for electronics: large-area growth of bilayer-free graphene on SiC, 2d Mater 3 (2016), 041002.
- [24] Y. Hu, M. Ruan, Z. Guo, R. Dong, J. Palmer, J. Hankinson, C. Berger, W.A.d. Heer, Structured epitaxial graphene: growth and properties, J. Phys. D Appl. Phys. 45 (2012), 154010.
- [25] C. Berger, E. Conrad, W.A. de Heer, Epigraphene, in: P.C. G. Chiarotti (Ed.) Physics of Solid Surfaces, Landolt Börstein encyclopedia Springer-Verlag, Germany, 2018, pp. 727-807. ArXiv:1704.00374.
- [26] C. Berger, D. Deniz, J. Gigliotti, J. Palmer, J. Hankinson, Y. Hu, J.-P. Turmaud, R. Puybaret, A. Ougazzaden, A. Sidorov, Z. Jiang, W.A. de Heer, Epitaxial Graphene on SiC: 2D Sheets, Selective Growth and Nanoribbons, in Growing Graphene on Semiconductors, Eds. N. Motta, C. Coletti, F. Iacopi, PanStanford publishers, DOI (2017) p181 (ArXiv:1611.08937).
- [27] A.C. Ferrari, J.C. Meyer, V. Scardaci, C. Casiraghi, M. Lazzeri, F. Mauri, S. Piscanec, D. Jiang, K.S. Novoselov, S. Roth, A.K. Geim, Raman spectrum of graphene and graphene layers, Phys. Rev. Lett. 97 (2006), 187401.
- [28] R.S. Pease, An X-ray study of boron nitride, Acta Crystallogr. 5 (1952) 356–361.
- [29] A. Henry, M. Chubarov, Z. Czigány, M. Garbrecht, H. Högberg, Early stages of growth and crystal structure evolution of boron nitride thin films, Jpn. J. Appl. Phys. 55 (2016) 05FD06.
- [30] K. Zhang, M. Arroyo, Understanding and strain-engineering wrinkle networks in supported graphene through simulations, J. Mech. Phys. Solids 72 (2014) 61–74.
- [31] K. Bera, D. Chugh, A. Patra, H.H. Tan, C. Jagadish, A. Roy, Strain distribution in wrinkled hBN films, Solid State Commun. 310 (2020), 113847.
- [32] D. Guan, W.M. Rainforth, L. Ma, B. Wynne, J. Gao, Twin recrystallization mechanisms and exceptional contribution to texture evolution during annealing in a magnesium alloy, Acta Mater. 126 (2017) 132–144.